Nanoscale

Cite this: *Nanoscale*, 2012, **4**, 2072

www.rsc.org/nanoscale

PAPER

Spatially resolved frequency-dependent elasticity measured with pulsed force microscopy and nanoindentation

Kim K. M. Sweers, Kees O. van der Werf, Martin L. Bennink* and Vinod Subramaniam*

Received 22nd December 2011, Accepted 2nd January 2012
DOI: 10.1039/c2nr12066f

Recently several atomic force microscopy (AFM)-based surface property mapping techniques like pulsed force microscopy (PFM), harmonic force microscopy or Peakforce QNM® have been introduced to measure the nano- and micro-mechanical properties of materials. These modes all work at different operating frequencies. However, complex materials are known to display viscoelastic behavior, a combination of solid and fluid-like responses, depending on the frequency at which the sample is probed. In this report, we show that the frequency-dependent mechanical behavior of complex materials, such as polymer blends that are frequently used as calibration samples, is clearly measurable with AFM. Although this frequency-dependent mechanical behavior is an established observation, we demonstrate that the new high frequency mapping techniques enable AFM-based rheology with nanoscale spatial resolution over a much broader frequency range compared to previous AFM-based studies. We further highlight that it is essential to account for the frequency-dependent variation in mechanical properties when using these thin polymer samples as calibration materials for elasticity measurements by high-frequency surface property mapping techniques. These results have significant implications for the accurate interpretation of the nanomechanical properties of polymers or complex biological samples. The calibration sample is composed of a blend of soft and hard polymers, consisting of low-density polyethylene (LDPE) islands in a polystyrene (PS) surrounding, with a stiffness of 0.2 GPa and 2 GPa respectively. The spring constant of the AFM cantilever was selected to match the stiffness of LDPE. From 260 Hz to 1100 Hz the sample was imaged with the PFM method. At low frequencies (0.5–35 Hz), single-point nanoindentation was performed. In addition to the material's stiffness, the relative heights of the LDPE islands (with respect to the PS) were determined as a function of the frequency. At the lower operation frequencies for PFM, the islands exhibited lower heights than when measured with tapping mode at 120 kHz. Both spring constants and heights at the different frequencies clearly show a frequency-dependent behavior.

1 Introduction

Atomic force microscopy (AFM) is widely used to study (bio) materials for their nanoscale morphological properties. Aside from these morphological studies AFM is also a suitable tool to characterize the mechanical properties of materials on the nanoscale.[1–3] Nanoindentation with an AFM tip is the most widely used method to determine nanomechanical properties of polymers.[4–6] In this mode the tip approaches and indents the sample until a certain predefined force is reached. At this point the tip is retracted. During this approach and retract cycle the force is continuously measured, resulting in a force *versus* distance graph, from which the modulus of elasticity can be derived using different contact models.[7–9] Besides the information in the force curve itself, the residual indentation depth measured with the AFM imaging mode could also be translated into hardness values of the polymers.[6,10]

The approach–retract cycle in nanoindentation is typically performed at a rate of 0.5 to 10 Hz, which makes this method inherently slow. Nanoindentation can also be used in a force–volume mode to get an overview of the mechanical properties of a sample. In this approach, a complete force curve is recorded for every pixel in an image, which results in data acquisition times of up to hours for a single image.

Recently several high-speed surface property mapping techniques like pulsed force microscopy (PFM), harmonic force microscopy and Peakforce QNM have been introduced.[11–13] These modes work on the same principle as the conventional nanoindentation approach but at far higher frequencies, leading to a significantly higher data throughput. These modes are used to obtain mechanical information on polymers,[11,14] and are also increasingly used on biological materials like DNA or amyloid proteins.[15,16]

Nanobiophysics, MESA+ Institute for Nanotechnology, Faculty of Science and Technology, University of Twente, Enschede, The Netherlands. E-mail: m.l.bennink@utwente.nl; v.subramaniam@utwente.nl

However, complex materials like polymers and biological materials are known to display viscoelastic behavior, a combination of solid- and fluid-like responses depending on the frequency at which the sample is probed.[17–19] In spite of this known behavior, very few AFM studies have attempted to characterize the frequency-dependent modulus of elasticity of complex materials. Kim *et al.* studied the response of PDMS, a polymer with a surface stiffness similar to that of biological samples, probed at different frequencies.[20] They clearly showed the viscoelastic response of PDMS within the frequency range of 1 Hz to 1000 Hz. Yang *et al.* demonstrated the viscoelastic behavior of poly(vinyl alcohol) nanofibers suspended over a channel.[21] A few studies on biological samples such as filaments or cells have also been performed,[22–24] but these studies have typically been limited to a small frequency range, mostly in the conventional nanoindentation frequency regime.

We use the AFM in nanoindentation mode and PFM mode to study the frequency-dependent behavior of low-density polyethylene (LDPE) using a standard 'training' sample supplied by Bruker (Bruker, Santa Barbara CA, USA). This sample is often used as a calibration sample for the surface property mapping techniques like Peakforce QNM or HarmoniX. A previous study showed that the elastic modulus of LDPE increases when probed between 0.5 Hz and 1000 Hz at room temperature.[25] Here we show that with increasing frequency, up to frequencies frequently used in methods such as PFM or Peakforce QNM®, the apparent stiffness (which is proportional to the elastic modulus) of the LDPE increases. This study demonstrates the ability, with the development of these new mechanical property mapping methods, to probe nanoscale rheological behavior of materials with AFM, at much broader frequency ranges than so far possible. Moreover, these results show that the frequency-dependent variations in mechanical properties of a sample like LDPE are very prominent in the frequency range used in these surface property mapping methods. Such samples should therefore be used with care for calibration purposes.

2 Materials and methods

Sample and tip

The sample consists of a surface of polystyrene (PS) with phase separated islands of low-density polyethylene (LDPE) spin coated on top of a silicon plate (HarmoniX training sample PS-LDPE, Bruker, Santa Barbara CA, USA). The PS layer has a thickness of 20–30 nm and has a bulk modulus of elasticity of 2 GPa. The LDPE islands are around 2000 nm in diameter and 30–45 nm thick and have a bulk modulus of elasticity of 0.2 GPa.

The sample is scanned and indented with an MSCT tip F cantilever (Bruker, Santa Barbara CA, USA). For both single-point nanoindentation and pulsed force microscopy experiments one single cantilever is used to compare the results. The nominal spring constant of this cantilever is 0.5 N m^{-1}, the nominal tip radius is 10 nm and the resonant frequency is around 120 kHz. This spring constant (or stiffness) of the cantilever is matched with the stiffness of the LDPE, in order to be sensitive for changes in the elastic properties of the LDPE. The stiffness of the PS however, is much higher compared to the cantilever spring constant, rendering this method insensitive for the elastic properties of the PS. This means that the PS layer is perceived to be as stiff as the silicon layer underneath. The stiffnesses extracted from the force curves recorded on the bare silicon substrate and the PS layer indeed did not show significant differences.

Single-point nanoindentation

A Bioscope Catalyst microscope (Bruker, Santa Barbara CA, USA) was used for the single-point nanoindentation experiments. The measurements were performed with the "point and shoot" application in the NanoScope 8.10 software. To locate the LDPE islands, we first imaged the sample in tapping mode. Thereafter, the tapping amplitude was set to zero and indentation curves were made in the TM deflection mode as implemented in the Nanoscope 8.10 software. The maximum force applied on the sample was on average around 10 nN. In total 5 curves each on the PS and on a LDPE drop were recorded at different frequencies, namely at 0.5 Hz, 1 Hz, 2 Hz, 5 Hz, 10 Hz, 20 Hz and 35 Hz. The slopes of the retract curves were determined by fitting a linear function to the data for the first 5 nm, ultimately resulting in average slopes for PS and LDPE. We used only the first 5 nm of the curve (that is, <20% of the sample thickness) to account for finite sample thickness effects.[26] At each measurement frequency, we then calculated the stiffness of LDPE.

Pulsed force microscopy

The pulsed force microscopy (PFM) method was used as implemented on a WITec alpha 300 microscope series (WITec alpha 300 microscope, WITec focus innovations, Germany). In the PFM method the cantilever is driven with a sinusoidal function and allows a maximum force setpoint; here a setpoint of 0.5 V (17.5 nN) was used. This force resulted in a maximum indentation, at the lower frequencies, of 3.5 nm, which is well under 20% of the total LDPE thickness. The cantilever is continuously in contact with the sample to avoid snap-in/snap-off effects due to adhesion forces, especially on the PS part of the sample. This gives direct control of the amplitude of the sinusoidal function (50–60 nm on PS). The software generates several images including error signal and topography, which are built up by measuring the z-stage displacement required to maintain the setpoint force. Three additional images are created by choosing three different user-defined regions in the sinusoidal signal (see Fig. 1A): a red region for the maximum force, a green region for the slope (called stiffness in the software) and a blue region for the minimum force to get information about the amplitude. Furthermore, it is possible on this microscope to change the drive frequency. A frequency range of 260 Hz to 1100 Hz with steps of 50 Hz was used to measure the sample. The average height and slope (representing the measured stiffness, or the contact stiffness) values for a large LDPE island were determined and compared to the direct PS surrounding of the island. With these values the stiffness of LDPE was calculated.

Modulus of elasticity values of LDPE from single-point nanoindentation

The raw deflection curves on LDPE, obtained on the Bioscope Catalyst AFM at 0.5 Hz and 10 Hz, were converted to a force separation curve using the deflection sensitivity of the cantilever

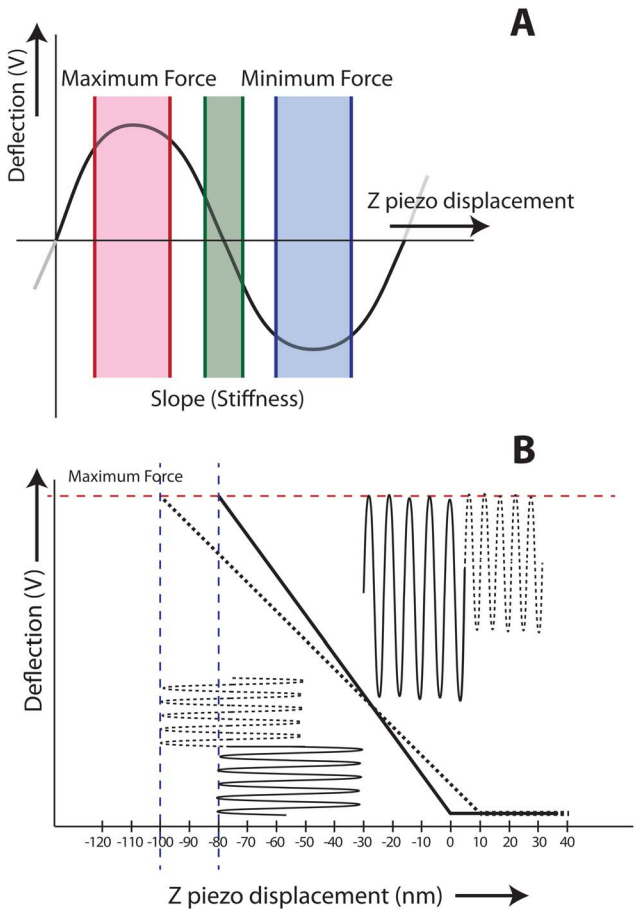

Fig. 1 PFM principle as implemented on a WITec alpha 300 microscope. Panel (A) shows the deflection signal with the three regions: maximum force (red area), slope (green area) and minimum force (blue area). The maximum force of the sine wave is the same as the force setpoint. The slope of the deflection in the green region is proportional to the measured stiffness (or contact stiffness) and changes as the elastic properties of the material being probed are changing. Panel (B) shows 2 force curves on both a hard sample (*e.g.*, PS, solid line) and a softer 10 nm higher feature (*e.g.* LDPE island, dashed line). The vertical sine wave represents the signal that is used for driving the cantilever and amplitude remains constant during the measurement. The resulting (measured) deflection signal is displayed horizontally and indicates a higher amplitude (steeper slope) on a hard sample compared to a soft sample. As the AFM tip indents the soft sample, the stage has to travel longer to reach the same force setpoint (the vertical blue lines indicate the z stage position), resulting in a lower height in the topography image and a smaller amplitude (or lower slope) indicating a softer material.

and the nominal spring constant provided by the manufacturer. The modulus of elasticity of LDPE was determined from the first 5 nm of the slope of the separation curve according to the DMT model,[2,8] using an estimated tip radius of 25 nm, a spring constant of 0.5 N m^{-1} and a Poisson ratio of 0.45.

3 Results

Fig. 2 shows two examples of the nanoindentation curves obtained at 0.5 Hz and 10 Hz. Both graphs show differences in the slopes of the curves corresponding to the LDPE and PS domains. The stiffness of LDPE is calculated with the following equation:

$$\frac{1}{k_t} = \frac{1}{k_c} + \frac{1}{k_s} \quad (1)$$

where k_t is the measured stiffness, k_c the cantilever stiffness (spring constant) and k_s the stiffness of the probed sample, here that of LDPE. From the curves shown in Fig. 2 the calculated LDPE stiffness changes from 0.18 N m^{-1} at 0.5 Hz to 0.46 N m^{-1} at 10 Hz. Applying the DMT model to the force separation curves measured at both frequencies yields modulus of elasticity of 349 MPa at 0.5 Hz and 787 MPa at 10 Hz.

Fig. 3 shows the images of the slope and height measured at different frequencies obtained with the WiTec AFM. The images of the slope clearly show a decreasing contrast between PS and LDPE at increasing frequencies. The slope on the PS stays constant due to the insensitivity of the chosen cantilever (see Materials and methods) for the stiff PS. This indicates that the material increases in stiffness with increasing frequency. In the topography images the height increase of the LDPE islands compared to the PS, as the frequency is increasing, is clearly visible. This height increase is caused by the implementation of the image method, that is, the cantilever needs to travel a longer distance on a soft sample (LDPE island) compared to a hard surface (PS) with a predefined force setpoint (Fig. 1B). At low frequencies, where the LDPE behaves as a soft material, the height signal is lower than the surrounding PS, due to the AFM tip sinking into the material. However, at higher frequencies, where the LDPE has a higher stiffness, the height signal corresponding to the LDPE is higher than that of the surrounding PS, and approaches values closer to the height measured in tapping mode (around 10 nm).

Fig. 4A shows the height increase of the LDPE islands compared to the surrounding PS measured with PFM, and also shows the actual height measured with tapping mode at 120 kHz. This graph shows the frequency-dependent effect already depicted in the image series of Fig. 3. The spring constants for LDPE calculated from the slopes of the curves acquired by both methods with eqn (1) are plotted *versus* frequency in Fig. 4C. For the stiffness calculations from the PFM results an area of interest is drawn on the LDPE island and the average spring constant of this area is used in eqn (1) to calculate the LDPE stiffness (Fig. 4D). The increase in stiffness with increasing frequency is clearly visible, even at lower frequencies (inset of Fig. 4C).

4 Discussion and conclusion

The graph in Fig. 4A, where the height measurements performed in PFM mode are combined with the actual height measured in tapping mode AFM, clearly shows the frequency-dependent behavior. The graph indicates that at lower operating frequencies the AFM measures the LDPE islands as being a softer material, resulting in the islands appearing as holes in the sample (Fig. 4B). The height measured with tapping mode AFM is commonly assumed to be the true height. In tapping mode, the cantilever essentially probes the sample at such a high frequency (120 kHz). At this frequency the material is extremely stiff, resulting in hardly any indentation under the applied force. These attributes

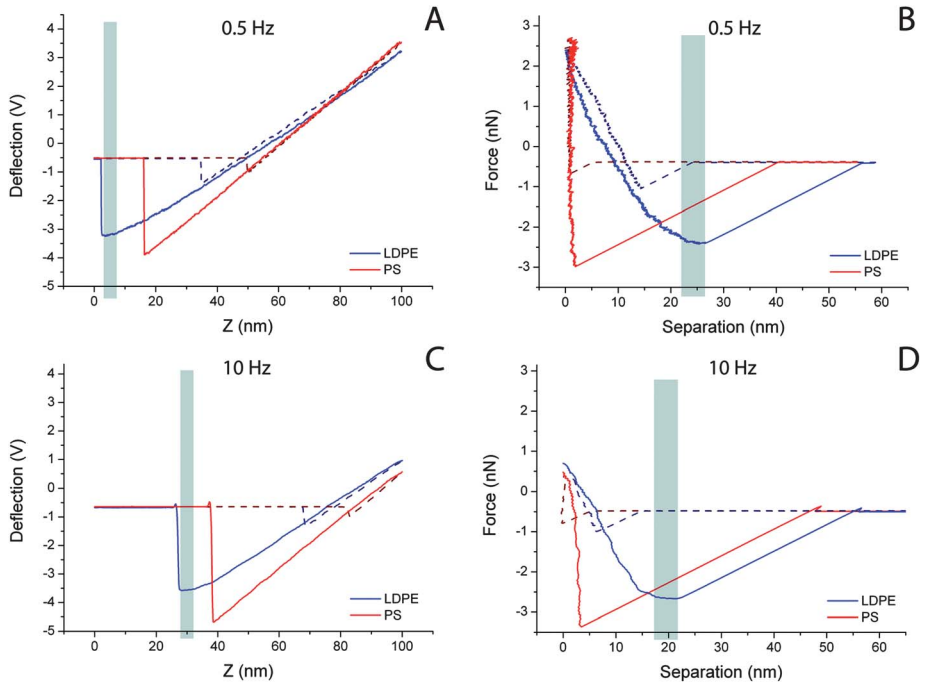

Fig. 2 Examples of the raw nanoindentation deflection curves at 0.5 Hz (A) and 10 Hz (C) and their corresponding force separation curves (B and D). Dotted and solid lines represent approach and retract curves respectively. Blue curves are measured on LDPE and red curves on PS. Due to indentation in a soft material and the finite-sample thickness effects the curves on LDPE are clearly not linear. Therefore the analysis of the raw deflection and separation curves is done on the first 5 nm (grey bars in graphs).

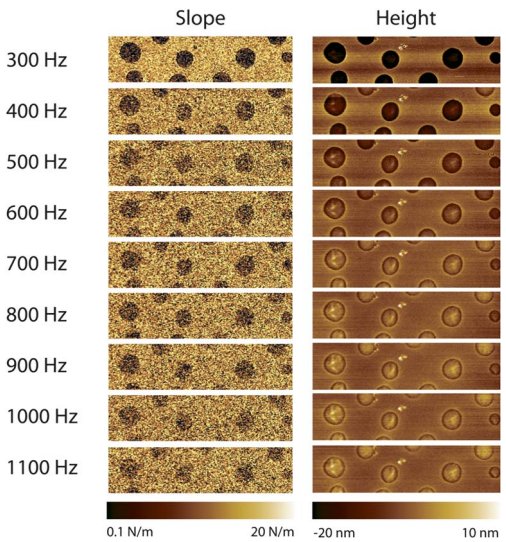

Fig. 3 Slope and topography images recorded with PFM at different frequencies. Image sizes are 10 × 2.5 μm. The contrast in the slope is very clear at low frequencies, whereas this contrast diminishes at higher frequencies. The heights of the LDPE islands are below the PS surface at the lower frequencies and gradually come up as the frequency is increased.

make it possible to gently image very soft and delicate samples, for instance live cells, using tapping mode imaging.[27]

While the height images made with PFM show very good contrast, the slope images have a low signal to noise ratio. For the height analysis presented here, we draw a line profile across the LDPE island and measure the difference between the PS background and the highest point of the LDPE island (Fig. 4B). The high noise level in the slope images made analyses of single line profiles difficult, and we thus chose to compute average values over a substantial area of an island (defined by the white circle in Fig. 4D) for the stiffness calculations.

Fig. 4C shows a clear dependence of the LDPE spring constant on the frequency. At the lowest frequency, 0.5 Hz, the LDPE spring constant is similar to the cantilever spring constant. Around 35 Hz the LDPE spring constant is already 5 times higher compared to the cantilever spring constant (see the inset of Fig. 4C). The gap in the data between 35 Hz and 260 Hz is attributed to instrumental limitations. Specifically, the PFM implemented in the WITec system was not capable of performing the measurements with the required force settings at operating frequencies below 260 Hz. Additionally, the nanoindentation software implemented on the Bioscope Catalyst automatically reduces the number of samples/pixels in the curve when measuring above 10 Hz. Above 35 Hz the number of pixels are reduced to less than 128 pixels, a value that appeared to be insufficient for robust analysis. At the higher frequencies, starting around 400 Hz, the LDPE stiffness approaches the maximum stiffness measurable with this particular cantilever. The stiffness measured on LDPE is related to the modulus of elasticity of LDPE, and the geometric contact volume of the probing tip. In this study we varied the force on the sample in contrast to bulk rheology measurements, in which the displacement is varied. We did not observe a distinct phase shift during the measurements, that is, no phase difference between the drive signal and the deflection signal. We used the same tip for the indentation

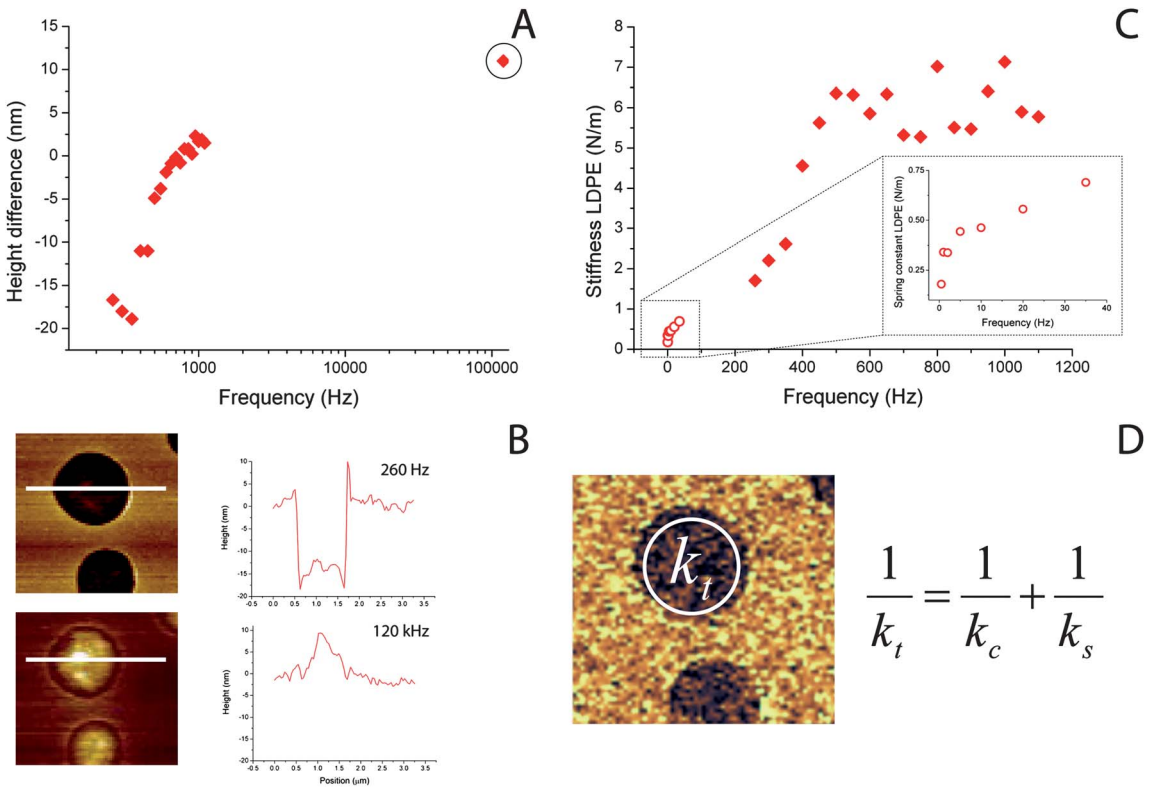

Fig. 4 Single-point nanoindentation and PFM results. (A) The height of a large LDPE island, compared to the PS surrounding, from the PFM images is plotted as a function of frequency. The circled data point depicts the height of the same island measured with tapping mode. (B) Examples of line profiles of the large LDPE islands at 260 Hz (upper image) and at tapping mode frequency of 120 kHz (lower image). (C) Frequency-dependent LDPE stiffness calculated from both single-point nanoindentation (open circle data points) and PFM measurements (filled diamond data points). Inset is a zoom of the single-point nanoindentation results at the lower frequencies. (D) Short description of the spring constant calculation method with the PFM results, where k_t is the total measured spring constant, k_c the cantilever spring constant and k_s the contact stiffness of the sample.

measurements, and indented only a few nanometres. From this we can conclude that this is pure elastic behavior and proportional to the storage modulus, G', of the LDPE. The G' of LDPE as a function of the frequency has been measured by Capodagli and Lakes using bulk rheology, and the frequency increase is in the same range as our results.[25] Future studies comparing this AFM technique with bulk rheology measurements of samples with the same thermal history should be done to get insights into whether absolute values of G' are in good agreement.

The modulus of elasticity values found for LDPE in this study are slightly higher compared to the provided value of around 200 MPa. However, the values we extract are in the same range as previous nanoindentation studies of LDPE.[6,28] Considering that the analysis of moduli of elasticity from contact models, like the DMT model used in this study, requires many assumptions on contact areas, point of contact, Poisson ratio and spring constant calibration methods,[2] we therefore chose to analyze our data only in terms of stiffness values. Also, since the LDPE islands are only 30–40 nm in thickness, the results are prone to finite sample thickness effects.[26,29] The maximal indentation on LDPE on the PFM measurements was 3.5 nm (less than 20% of the full thickness). For the single-point nanoindentation measurements we only used the first 5 nm of the curve for analysis. To exclude that the frequency-dependent behavior measured here is induced by plastic deformation caused by the multiple scans, the sample was scanned in PFM mode at 260 Hz for multiple times in the same time span as the variable frequency series. However, there was no effect seen in the height images during a 70 minute time span (Fig. 5), confirming that the results shown in Fig. 3 are indeed attributable to a purely elastic effect which is frequency-dependent.

We observed an increase in the LDPE stiffness within 400 Hz. This increase and the repeated measurements at one frequency show that results obtained at a certain frequency could be very reproducible (Fig. 5), but that they are completely different when compared to the results measured at different frequencies. For LDPE this apparent stiffness already increases by a factor of 2 when going from 0.5 Hz to 2 Hz. It is thus crucial to report the frequency at which nanomechanical properties are measured for effective comparison of experimental data. The shape of the stiffness curve obtained here is specific for the LDPE material.[25,30]

High speed surface property modes are often calibrated with a training sample composed of copolymer blends, such as the LDPE/PS blend used here. The LDPE component of this sample is very soft and proven to be very frequency-dependent. This polymer is used in the calibration sample because the modulus of elasticity is close to the moduli of elasticity of biological samples. However the question remains whether the frequency-dependent behavior is also comparable to other polymers and especially to biological materials. The new surface property mapping methods probe at very high frequencies compared to the conventional

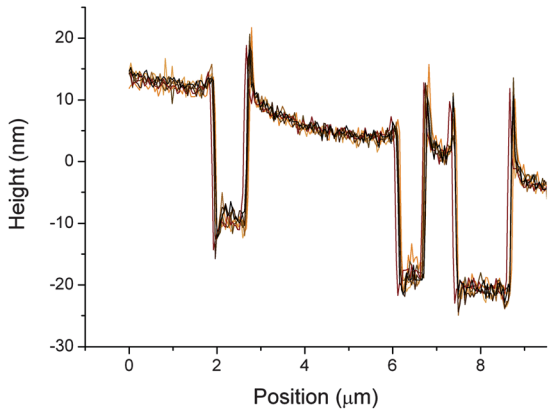

Fig. 5 Line traces of 7 topographic images made with the PFM method in a period of 70 minutes at 260 Hz with similar settings as the frequency series. The traces show no height increase as seen in Fig. 3, which confirms that the results shown in Fig. 3 are truly frequency-dependent.

nanoindentation technique. Although the data throughput is very fast, one should combine the results with nanoindentation measurements at low frequencies. In this manner the frequency-dependent behavior of the sample, which could influence the measurement and analyses, can be studied. Furthermore, it is very important to calibrate the measurement system with a calibration sample which exhibits elastic and viscoelastic behaviors that are close to those of the actual sample to be measured. The results obtained in this study show that frequency-dependent behavior of a sample like LDPE is very prominent in the frequency range used in the recently developed surface property mapping methods. These approaches should be calibrated with the deflection sensitivity, spring constant and tip radius of the cantilever instead of with the training samples alone. Finally, all mechanical properties measured with these surface property mapping techniques or with conventional nanoindentation should be reported with explicit mention of the frequency at which the sample is probed.

In this study we have shown that in addition to measuring morphological and elasticity properties, AFM is also very well suited to investigate frequency-dependent behavior of complex materials. The results obtained are very similar to those from bulk rheological studies,[25,30] with the added advantage of being able to spatially resolve these properties at exceedingly small length scales. Although a few studies on nano/micro-rheology using AFM exist, they are still limited to narrow frequency ranges, often below 100 Hz.[24,31,32] We demonstrate that, with the development of the new nanomechanical mapping techniques, AFM can be used to obtain frequency-dependent modulus of elasticity curves of nanometre sized single polymer or biological samples in considerably larger frequency ranges, which are not accessible to conventional rheology.

References

1 L. Yang, K. O. van der Werf, B. F. J. M. Koopman, V. Subramaniam, M. L. Bennink, P. J. Dijkstra and J. Feijen, *J. Biomed. Mater. Res., Part A*, 2007, **82A**, 160–168.
2 K. Sweers, K. Werf, M. Bennink and V. Subramaniam, *Nanoscale Res. Lett.*, 2011, **6**, 270.
3 T. P. J. Knowles and M. J. Buehler, *Nat. Nanotechnol.*, 2011, **6**, 469–479.
4 S. Bhuyan, S. Sundararajan, D. Andjelkovic and R. Larock, *Tribol. Int.*, 2010, **43**, 2231–2239.
5 E. Celik, E. Oterkus, I. Guven and E. Madenci, *IEEE*, 2009, 262–268.
6 A. Y. Jee and M. Lee, *Polym. Test.*, 2010, **29**, 95–99.
7 H. Hertz, *Reine Angew. Math.*, 1882, **94**, 156–171.
8 B. V. Derjaguin, V. M. Muller and Y. P. Toporov, *J. Colloid Interface Sci.*, 1975, **53**, 314–326.
9 K. L. Johnson, K. Kendall and A. D. Roberts, *Proc. R. Soc. London, Ser. A*, 1971, **324**, 301–313.
10 D. Tranchida, Z. Kiflie and S. Piccarolo, *Macromolecules*, 2007, **40**, 7366–7371.
11 B. Pittenger, N. Erina, C. Su, Application Note Veeco Instruments Inc. http://nanoscaleworld.bruker-axs.com/nanoscaleworld/media/p/418.aspx.
12 A. Rosa-Zeiser, E. Weilandt, S. Hild and O. Marti, *Meas. Sci. Technol.*, 1997, **8**, 1333–1338.
13 O. Sahin, *Rev. Sci. Instrum.*, 2007, **78**, 103707.
14 P. Schön, K. Bagdi, K. Molnár, P. Markus, B. Pukánszky and G. J. Vancso, *Eur. Polym. J.*, 2011, **47**, 692–698.
15 O. Sahin and N. Erina, *Nanotechnology*, 2008, **19**, 445717.
16 M. Dong, S. Husale and O. Sahin, *Nat. Nanotechnol.*, 2009, **4**, 514–517.
17 Y. C. Nho, J. I. Kim and P. H. Kang, *J. Ind. Eng. Chem.*, 2006, **12**, 888–892.
18 J. Meissner, *Pure Appl. Chem.*, 1975, **42**, 551–612.
19 A. K. Van der Vegt, *Polymeren, van keten tot kunststof*, Delft University Press, 1999.
20 K. S. Kim, Z. Lin, P. Shrotriya, S. Sundararajan and Q. Zou, *Proc. 3rd Ann. IEEE Conf. Aut. Sci. and Eng.*, 2007, SuRP-B02.1, pp. 219–224.
21 N. Yang, K. K. H. Wong, J. R. Bruyn and J. Hutter, *Meas. Sci. Technol.*, 2009, **20**, 025703 (9p).
22 O. Chaudhuri, S. H. Parekh and D. A. Fletcher, *Nature*, 2007, **445**, 295–298.
23 T. P. J. Knowles, T. W. Oppenheim, A. K. Buell, D. Y. Chirgadze and M. E. Welland, *Nat. Nanotechnol.*, 2010, **5**, 204–207.
24 K. E. Bremmel, A. Evans and C. A. Prestidge, *Colloids Surf., B*, 2006, **50**, 43–48.
25 J. Capodagli and R. Lakes, *Rheol. Acta*, 2008, **47**, 777–786.
26 R. M. A. Sullan, N. Gunari, A. E. Tanur, Y. Chan, G. H. Dickinson, B. Orihuela, D. Rittschof and G. C. Walker, *Biofouling*, 2009, **25**, 263–275.
27 C. A. J. Putman, K. O. Van der Werf, B. G. de Grooth, N. F. Hulst and J. Greve, *Biophys. J.*, 1994, **67**, 1749–1753.
28 D. Passeri, A. Bettucci, A. Biagioni, M. Rossi, A. Alippi, M. Lucci, I. Davoli and S. Berezina, *Rev. Sci. Instrum.*, 2008, **79**, 066105.
29 S. Guo and B. B. Akhremitchev, *Biomacromolecules*, 2006, **7**, 1630–1636.
30 M. Yamaguchi and S. Abe, *J. Appl. Polym. Sci.*, 1999, **74**, 3160–3164.
31 R. E. Mahaffy, C. K. Shih, F. C. MacKintosh and J. Käs, *Phys. Rev. Lett.*, 2000, **85**, 880–883.
32 P. Roca-Cusachs, I. Almendros, R. Sunyer, N. Gavara, R. Farré and D. Navajas, *Biophys. J.*, 2006, **91**, 3508–3518.